Acta Avionica
Volume XVII, 31 – No.1, 2015

EXPERIMENTAL VERIFICATION OF UNSTABLE CENTRIFUGAL COMPRESSOR WORK ON SMALL JET ENGINE

Marián HOCKO
Hocko Marián, Ing., PhD., Faculty of Aeronautics Technical University of Košice
Rampová 7, 041 21 Košice Slovakia
e-mail: marian.hocko@tuke.sk

Summary. The article, based on practical experiments, analyzes the process of creating an unstable operation of a centrifugal compressor (surge) because of throttling the air flow into the inlet device. The aim of the article is to provide information on preparation, methodology and results of the experiments that were carried out in the research of unstable phenomena in a centrifugal compressor MPM-20 in the Laboratory for small turbojets engines that is a part of the Department of Aviation Engineering at the Faculty of Aeronautics, Technical University of Kosice, Slovak Republic. The knowledge gained from the above experiments allow improved understanding of both birth and development processes of unstable work in radial compressors, thereby preventing such phenomena in the real operation of air turbo-compressor engines (ATCE) and gas turbines (GT). The consequences of unstable work were analyzed on the damaged gas turbine.

Keywords: unstable work of an centrifugal compressor, experimental small jet engine, surge

1. INTRODUCTION

Unstable work (surge) of compressors is a dangerous phenomenon that occurs in a particular mode of compressors of ATCE and also GT that are used in vehicles and stationary applications. That is manifested by sudden changes in pressure and speed of the airflow at the outlet of the compressor and by characteristic sound effects that give rise to intense vibrations of the rotor blades and by changes of the of air flow characteristics in other parts of both ATCE and GT. The consequences of unstable work of the compressor are associated with cessation of activities of ATCE and GT, or their destruction because of mechanical damage of the compressor blades or destruction (burning) of the gas turbine blades. Therefore, the formation of unstable work of the compressor is inadmissible and much attention is devoted to prevention of its starting in ATCE and GT.

Carrying out the research in unstable work of ATCE and GT compressors in a real operational context is associated with potential security risks and significant economic costs due to damage or destruction of expensive engines. Relevant results can be achieved without the mentioned risks under the laboratory conditions using the experimental small turbojet engine MPM - 20 that were created by transforming the turbine trigger TS - 20 into a small single jet engine. In experiments conducted at the Department of Aviation Engineering at the Faculty of Aeronautics, Technical University of Kosice, artificially induced unstable work of a centrifugal compressor, virtually confirmed the hypotheses and the relevant consequences for particular parts of the engine [1].

2. LAUNCH MECHANISM OF UNSTABLE COMPRESSOR WORK

Unstable work of the ATCE compressor is a phenomenon that occurs when a particular mode of work of the compressor is manifested by severe periodic changes in the air flow rate $\mathbf{Q_{air}}$, the output pressure $\mathbf{p_2}$, absolute air speed $\mathbf{c}$ and sometimes back-flow of air from the compressor to the input. Concomitants of unstable work of the ATCE compressor are:

- pulsation of pressure and air velocity at the outlet of the compressor,
- a reduction of the mean pressure at the outlet of the axial compressor $\mathbf{p_{2,\,centr}}$.
- characteristic sound effects,
- engine vibration,
- vibration of compressor rotor blades.

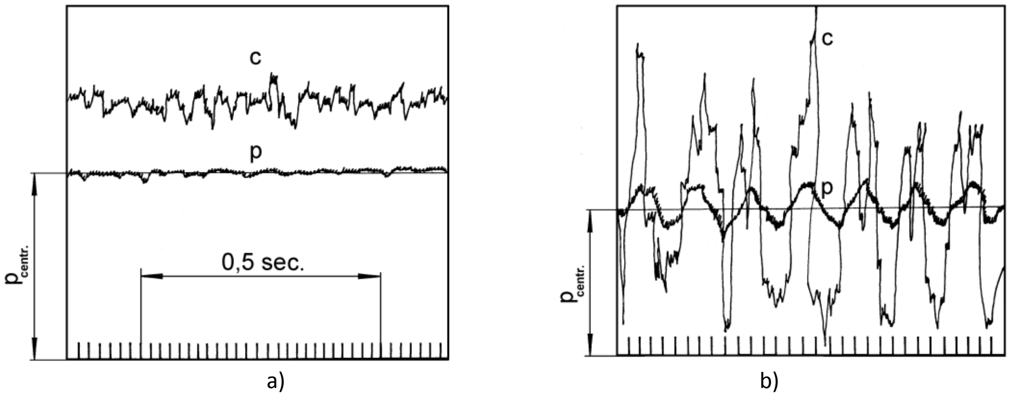

Figure 1: Recorded parameter changes as the compressor is in surging [2]
a – stable work of compressor, b – unstable work of compressor

The formation of unstable compressor work during the operation of ATCE or GT can occur for various reasons, for example as a consequence of:
- unstable work of input ATCE or GT device,
- failures of an engine control system (accelerator machine, high-pressure pump, etc.),
- sucking an object (birds, ice, etc.),
- sudden changes in temperature conditions at the inlet to the engine (while passing over the fire, active volcano or sucking the off-gasses of another aircraft or launched missiles, etc.),
- sudden changes in active areas of the input device of the engine when aircraft is maneuvering,
- changes in air quality, for example in sucking volcanic ash volcanic when flying in the volcanic cloud and the like.

The consequence of unstable work of the ATCE or GT compressors can be:
- an irregular operation of the engine,
- a reduction in thrust (power) owing to reduced flowing amount of air through the engine,
- distortion of the normal steady burning of fuel-air mixture in the combustion chamber of ATCE,
- the sharp increase in gas total temperature in front of the gas turbine ATCE $\mathbf{T_{3t}}$,
- increase of the vibration level of the whole ATCE,
- possibility of breakage of the ATCE compressor rotor blades because of vibration.

Regarding the accompanying phenomena, which may lead to an interruption of the engine, its damage, or destruction of unstable work of the compressor, is admissible [5].

The entire process of creating the unstable work of the ATCE compressor is rather complicated. The physical principle to form unstable compressor work is based on tearing streamlines of airflow at the run around an individual compressor blade when major departure from the calculation mode of operation of the compressor, resulting in a sudden change in the air supply and pressure conditions at the inlet of the compressor ATCE.

3 LAUNCH OF UNSTABLE WORK OF A CENTRIFUGAL COMPRESSOR

In operation, the centrifugal compressor in a computing mode corresponds to the air flow rate $\mathbf{Q_{air}} = \mathbf{Q_{air,\,cal.}}$ of the rotor speed $\mathbf{n}$ and the peripheral speed of the rotor $\mathbf{u_1}$ at the absolute inlet air velocity $\mathbf{c_{1a}}$ specifies the initial relative air speed at the rotor blade inlet $\mathbf{w_1}$, which flows in the direction of a tangent towards the central curve profile of a rotor blade to in between rotor blade channel. The outlet absolute velocity of the air from the compressor rotor blade $\mathbf{c_2}$ enters in diffuser. The airflow through the centrifugal compressor is smooth, without creating turbulence. The radial compressor is stable (Fig. 2a).

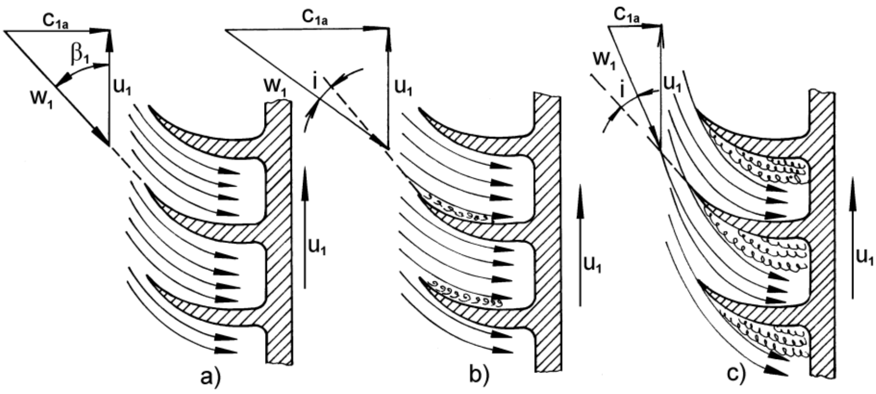

Figure 2 The airflow character of an axial compressor stage

With an increase in the rate of airflow $\mathbf{Q_{air}} > \mathbf{Q_{air,\ cal.}}$, and the particular rotor speed **n** the circuit rotor speed $\mathbf{u_1}$ will create, with the increased absolute speed $\mathbf{c_{1a}}$, a resulting input relative velocity of the air at the entrance to the rotor blades $\mathbf{w_1}$ the direction of which will deviate from the direction of the tangent to the profile middle curve of the rotor blade. This will cause hindering the smooth laminar airflow in the riverbed of rotor blades. The turbulent flow in the riverbed of blades will decline and there will be no farther spread of the breakaway streamlines into diffuser of the centrifugal compressor. Therefore, in this case there will be no formation of unstable work of the ATCE centrifugal compressor (Fig. 2b).

In reducing the rate of airflow $\mathbf{Q_{air}} < \mathbf{Q_{air,\ cal.}}$ and particular engine speed **n**, the circuit rotor speed **u** will create, with reduced absolute speed $\mathbf{c_{1a}}$, the resulting relative speed $\mathbf{w_1}$ the direction of which will deflect from the tangent to the medium curve of a rotor blade profile. This disrupts the smooth rotor blade and on their backs tearing off streamlines will occur and laminar flow to turbulent flow will be converted and spread farther to the diffuser vanes of the centrifugal compressor. The roiled air flow in a centrifugal compressor reduces smooth air flow farther into the main combustion chamber of the ATCE; it will result in backward flow of air back towards the ATCE input device. So the back flow of air in the space in front of the main combustion chamber sharply reduces air pressure and the air starts to move away from the input device to the main ATCE combustion chamber. The unstable air flow (surge) through the ATCE centrifugal compressor results in an abrupt change in the composition of the fuel-air mixture in the main combustion chamber which causes a significant increase in the overall total temperature of the gas in front of the gas turbine $\mathbf{T_{3t}}$ (sparingly rich mixture of fuel and air) and vibration of the rotor blades of the axial compressor with the possibility of their damage due to fatigue fracture (Fig. 2c).

The formation of unstable work of the ATCE centrifugal compressor usually occurs at higher values of calculated speed $\mathbf{n_p}$, such as computing speed mode $\mathbf{n_{p,\ cal.}}$.

$$n_p = n.\sqrt{\frac{288}{T_{1t}}}\ \left[\min.^{-1}\right]$$
$$n_p = n.\sqrt{\frac{288}{T_1.\left(1+\frac{\kappa-1}{2}.M_1^2\right)}}\ \left[\min.^{-1}\right] \tag{1}$$

where: $\mathbf{n_p}$ - converted speed [min^{-1}], **n** - measured speed of rotation [min^{-1}], $\mathbf{T_{1t}}$ - the total air temperature at the inlet to the centrifugal compressor [K], $\mathbf{T_1}$ - static air temperature at the inlet to the centrifugal compressor [K], **M** - Mach flight number [1].

The equation (1) shows that the calculated speed will increase at low static air temperature $\mathbf{T_1}$ and low speed expressed in the figure $\mathbf{M_1}$, corresponding to activities of ATCE in climbing to a great height.

If the air flow rate through a centrifugal compressor equals to the computational rate of air flow $\mathbf{Q_{air}} = \mathbf{Q_{air,\ cal.}}$, the airflow of centrifugal compressor blades and diffuser vanes is smooth, the unstable work of a centrifugal compressor will not occur. The centrifugal compressor will work stably (Fig. 2a).

If the air flow rate through a centrifugal compressor is greater than the calculated air flow rate $\mathbf{Q_{air}} > \mathbf{Q_{air,\ cal.}}$ tearing off the air flow in the riverbed of a centrifugal compressor blades will occur. As the tearing area of the air flow is relatively small, it does not spread. On the diffuser vanes the air flow is tearing off on the back of the blades. Air particles tend to move along the curves that are close to the logarithmic spirals. Roiling of the air flow reduces the efficiency of centrifugal compressor, but the air stream flows through the radial compressor but unstable work of the compressor usually does not occur (Fig. 3).

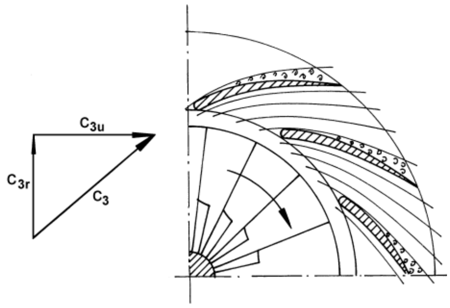

Figure 3 Tearing off the air streamlines on the back of diffuser vanes at $Q_{air} > Q_{air,\ cal.}$

In reducing the rate of air flow through a centrifugal compressor below the calculated amount of air $\mathbf{Q_{air}} < \mathbf{Q_{air,\ cal.}}$, tearing off the airflow at the back of the impeller blades (Fig. 2c) and diffuser vanes will occur (Fig. 4). The detached air stream loses velocity and reduces the flow area. So the decrease in the kinetic energy tends to increase the static pressure, which leads to the return flow and the consequent restoration of steady flow (surge). This process is again repeated at short intervals [2, 3].

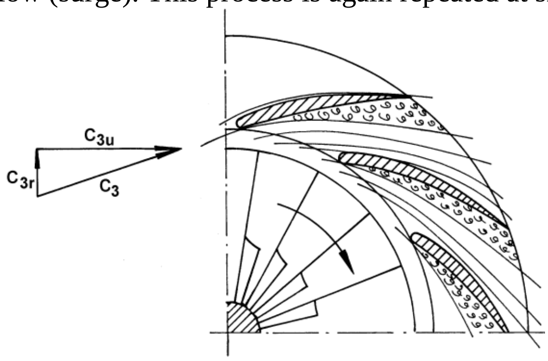

Figure 4 Tearing off the air streamlines on the back of diffuser vanes at $Q_{air} < Q_{air,\ cal.}$

4 EXPERIMENTAL VERIFICATION OF UNSTABLE WORK OF A CENTRIFUGAL COMPRESSOR

As mentioned in the previous part of this article, one of the causes of ATCE compressor unstable work is a change of air flow through the engine inlet device as a result of throttle down from variety of reasons. In theory, this process is explained in the particular (constant speed) mode by shifting an operating point along the line **n = const.** in the characteristics of a centrifugal compressor to the left border of the unstable work [4]. In sufficient reduction in air flow rate $\mathbf{Q_{air}}$ via the input device the operating point of the engine exceeds a threshold of unstable work and gets in unstable work of the centrifugal compressor (surge area) (Fig. 5)

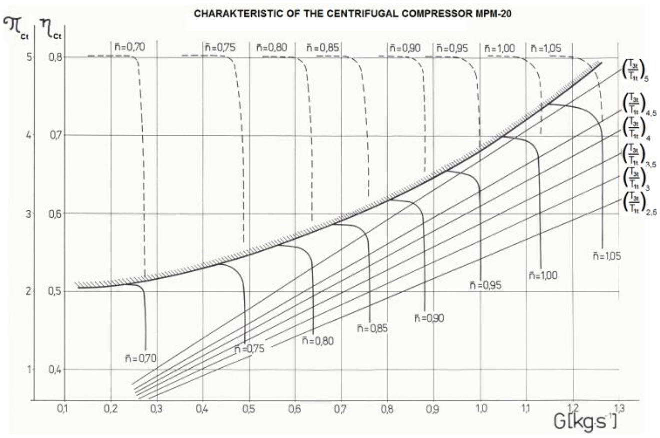

Figure 5 Calculated characteristics of a centrifugal compressor of an experimental engine MPM-20 [1, 4]

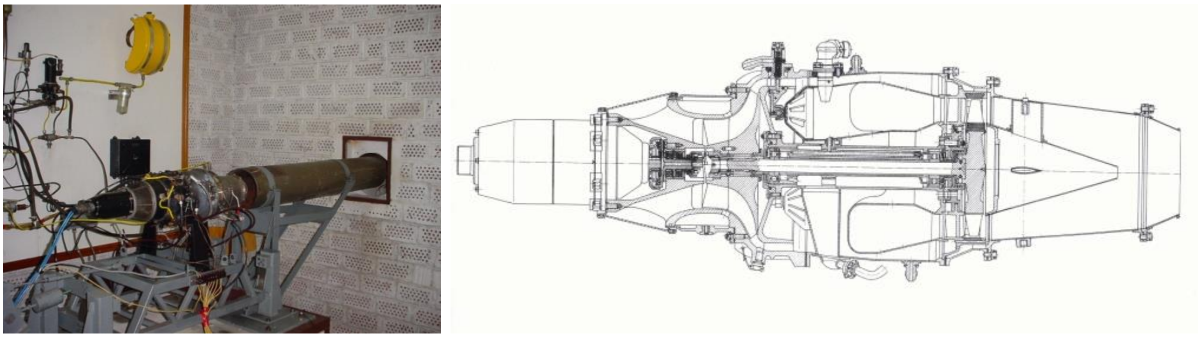

Figure 6 View of the MPM-20 at the Laboratory of small jet engines

For practical testing of theoretical hypotheses, the Laboratory for small turbojets at the Department of Aviation Engineering, Technical University of Kosice has been used, in which the experimental small single jet engine is available, it was created by conversion of the turbine trigger TS-20 [7].

MPM-20 is a small single jet engine with a diagonal entry system, single-stage centrifugal compressor, an associated combustion chamber, single stage uncooled gas turbine and fixed output nozzle.

The practical experimental verification of the impact of throttling the flow of air in the intake device of MPM - 20 on an unstable work of a centrifugal compressor, the method for gradual increasing the density of nets has been implemented; each was placed on the input system of the engine.

The processed linear mathematical model of MPM-20 is based on the theory of small changes in [8], described in [1, 10] for the sub-critical conditions of flow in the outlet nozzle, defines the conditions of change in the intake device reflected by changes of all parameters of the working process of single jet ATCE. For practical validation of this theory four sets of experimental measurements were prepared and aimed at gradually throttling the air flow through the input device MPM - 20th. The measured parameter values for individual experimental measurements are compared with the values obtained in the calibration measurement and the theoretical calculation based on the theory of small changes. Gradually these experimental measurements were realized:

1. Air flow through the input device of MPM - 20 without the input sieve.
2. Air flow through the input device of MPM - 20 with the sieve mesh size of 1.5 x 1.5 mm.
3. Air flow through the inlet system of MPM - 20 with a double sieve (a sieve with a mesh size of 1.5 x 1.5 mm and a sieve with mesh of 2.5 x 2.5 mm).
4. Air flow through the inlet device of MPM - 20 with a TV viewing screen with openings with a diameter of 0.4 mm.

The change in the independent variable (failures) was calculated according to the formula:

$$\delta X_{si} = \left[\frac{X_{si} - X_0}{X_0} \right] .100 [\%] \tag{2}$$

where: δX_{si} – change in the independent variable, X_{si} – a value parameter in a simulated malfunction, X_0 – an original value of the independent variable.

The change in the dependent variable value was calculated according to the equation:

$$\delta Y_{si} = \left[\frac{Y_{si} - Y_0}{Y_0} \right] .100 [\%] \tag{3}$$

where: δY_{si} – a change of the dependent variable, Y_{si} – a value parameter in the simulated malfunction, Y_0 – an original value of the dependent variable.

4.1 The airflow through the inlet device of MPM-20 without an inlet sieve

For the conditions of the first experiment the original input protective sieve was removed from the entrance system of MPM - 20.

Before carrying out the planned experiments, the MPM - 20 was set according to the technical documentation for a calculation scheme [9]. Subsequently 10 measurements of calibration parameters were performed. The mean value of the measured parameters obtained by the calibration measurement served as a benchmark for assessing changes in subsequent experimental measurements.

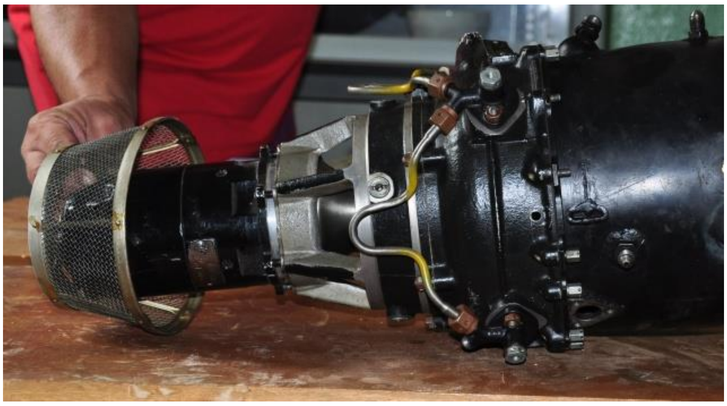

Figure 7 Removing the protective sieve from MPM-20

Table 1 Comparison of calculated and measured values of the parameters in the calibration measurements

PARAMETER	p_H	T_H	ACTIVITY PERIOD	$p_{2,K}'$	$p_{2t,K}'$	p_{2t}
UNIT	Pa	K	seconds	Pa	Pa	Pa
MEASURED VALUE	99885,82	290,65	50,8	180787,9	392652,7	351971,5
COUNTED VALUE	101325,2	288	50	181600,13	398549,2	392321,5
PARAMETER	p_3	p_4	T_{2t}'	T_{2t}	T_{3t}	T_{4t}
UNIT	Pa	Pa	K	K	K	K
MEASURED VALUE	351326,2	154655,78	458,55	460,25	1170,35	1043,45
COUNTED VALUE	392321,5	162812,95	462,35	462,35	1168,15	1013,27
PARAMETER	Q_{fuel}	G_{fuel}	c_h	F_T	G_{air}	c_m
UNIT	cm^3/CYCLE	kg/ CYCLE	$kg.h^{-1}$	N	$kg.s^{-1}$	$kg.h^{-1}.N^{-1}$
MEASURED VALUE	1362	1,05572	74,87	-	-	-
COUNTED VALUE	-	-	-	698,09	1,2	0,1311

A relatively high degree of agreement of measured and calculated thermodynamic parameters is apparent from the results of the calibration measurements processed in MPM - 20 and its comparison with the results of thermodynamic calculation of heat circulation of MPM - 20. Minor deviations between measured and calculated values of the thermodynamic parameters are caused by irregularities occurring in the measurement because of the location of sensors in other positions as suggested in the theoretical calculation.

In the first experiment (Fig. 7) 10 measurements were performed and the same parameters as for the calibration measurements MPM - 20 in the original configuration (with a protective sieve) were measured and evaluated. The mode of MPM - 20 operations was set to values that correspond to the calibration measurement (computing) mode; external conditions ($\mathbf{p_H}$, $\mathbf{T_H}$) have not changed.

As is apparent from the data given in [1], that compares the measured values of the parameters in the experimental measurements without the input sieve and the calibration measurements, the differences in individual parameters are minimum and range from -5.4 % (static gas pressure for gas turbine $\mathbf{p_4}$) to +2.9 % (total gas temperature for gas turbine $\mathbf{T_{4t}}$). Most of the other observed parameters have hardly changed even though the flow area of the inlet to the MPM - 20, after the removal of the inlet sieve, grew by 35 % (a total area of the inlet sieve with a wire sieve of a mesh size of 2.5 x 2.5 mm and wire thickness of 0.6 mm wire is 0.078593 m^2).

The results obtained by direct measurement of MPM - 20 without input sieve confirm that the choice of the wire diameter and the mesh size has been optimized by the engine manufacturer so that the sieve provides the protection from sucking strange objects with a minimum influence on the parameters of MPM – 20. Based on the measured parameters, the calculation of thrust $\mathbf{F_T}$ and of specific fuel consumption $\mathbf{c_m}$ were performed.

4.2 The airflow through the inlet device of MPM - 20 with the soft inlet sieve

In the second experimental measurement, the air flow through the soft sieve of an input device was throttled, which was deployed on the input device of MPM - 20. The total area of the inlet sieve is 0.078593 m^2. When using a wire sieve with a mesh size of 1.5 x 1.5 mm and a thickness of 0.3 mm wire, the occupied area of the input wire sieve is 34.984% of the total area of the input device.

The measured values of parameters of MPM - 20, described in [1], are very close to the measured values in calibration measurements with the original sieve.

4.3 Airflow through the inlet device of MPM - 20 with a double input sieve

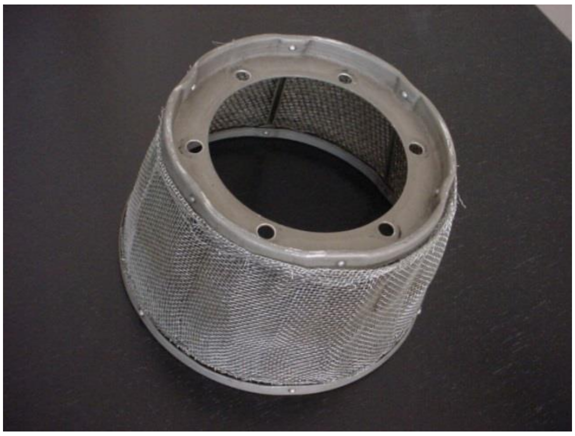

Figure 8 Dual sieve of MPM - 20

Third, experimental measurements were carried out at throttling of flow with the dual sieve (Fig. 8). To the original input device with an original protective sieve of MPM - 20 a soft sieve with the mesh size of 1.5 x 1.5 mm and a thickness of 0.3 mm wire was deployed, thus reducing the flow area by 58 %. On the basis of the reduction in the flow area of the inlet system the measured thermodynamic parameters have been changed, resulting in a change of the engine-dependent parameters. The total degree of gas expansion significantly changed on the gas turbine $\boldsymbol{\pi}_{\mathbf{Tt}}$ (about 19.194 %) and the total temperature of gas behind the gas turbine $\mathbf{T_{4t}}$ (by 4.475 %).

4. 4 Airflow through the inlet device of MPM - 20 with the sofest inlet sieve

The recent experimental measurement was carried out with strong throttling of flow through the input device, using a perforated metal plate with round holes 0.4 mm (a metal plate was originally used as a color TV viewing screen) (Fig. 9). The perforated plate was placed on the original sieve of an input device, thereby allowing a reduction by 83 % in the flow area of the inlet system of MPM - 20. This reducing of the flow area of the engine inlet device was substantial degradation of measured parameters compared to measured parameters at the input device without the inlet sieve ($\mathbf{\Delta p_{2t}}$ = -48 978.8 Pa, $\mathbf{\Delta p_3}$ = 24198.5Pa, $\mathbf{\Delta p_4}$ = -24957.82Pa, $\mathbf{T_{2t}}$ = -11.6K, $\mathbf{\Delta T_{3t}}$ = -92.4K, $\mathbf{\Delta T_{4t}}$ = -177.5 K, $\mathbf{c_h}$ = -4.3465kg.h^{-1}, $\boldsymbol{\Delta\pi}_{\mathbf{Tt}}$ = 0.6, $\boldsymbol{\Delta\pi}_{\mathbf{Ct}}$ = -0.509 a $\boldsymbol{\Delta\pi}_{\mathbf{JN}}$ = -0.257.

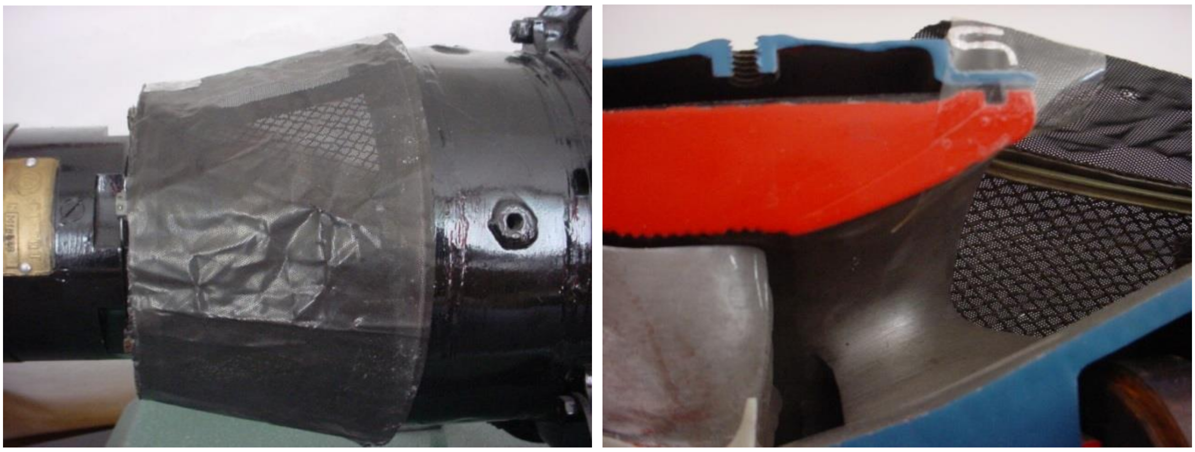

Figure 9 Perforated plate attached to the original inlet device of MPM-20

The seventh measurement with 83 % shading of the input device was in an unstable work of a centrifugal compressor of the engine and the destruction of gas turbine blades and to burn the sealant mass in the body of the gas turbine above rotor blades (Fig. 9).

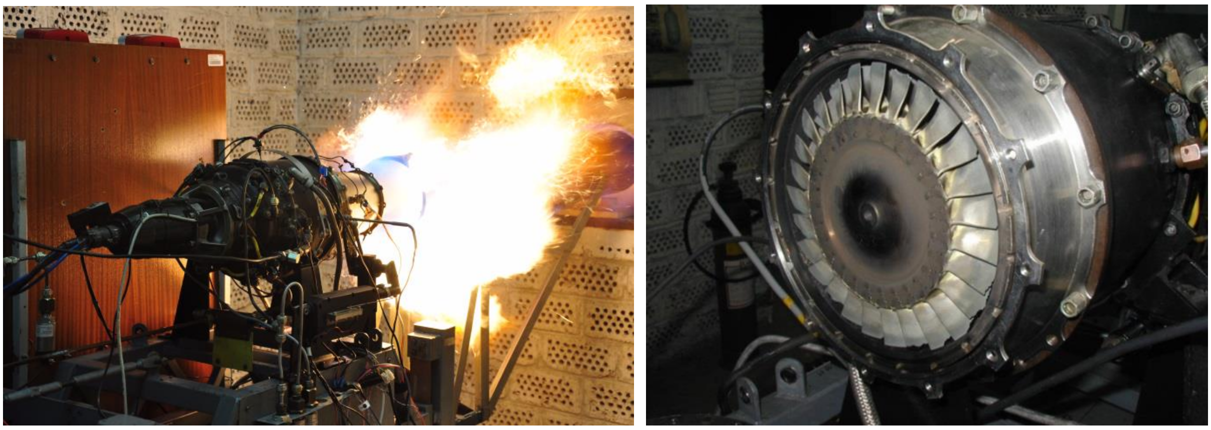

Figure 10 Destroyed gas turbine rotor blades of MPM - 20 because of unstable work of a centrifugal compressor (foto F. Adamčík, jun.)

Figure 11 Burned sealant in the body of the gas turbine rotor blades

5 CONCLUSIONS

Table 2 Result of the experimental measurements

PARAMETER	$S_{inlet.}$	p_H	T_H	Activity period	$p_{2,C}'$	$p_{2t,C}'$
UNIT	%	Pa	K	second	Pa	Pa
Inlet device without a sieve	100	100525.3	288.75	51.0	178967.1	388941.8
Inlet device with a soft sieve	80	100365.6	290.95	49.7	179136.7	390028.1
Inlet device with a basic sieve	65	99885.8	290.65	51.7	180787.9	391185.7
Inlet device with a dual sieve	58	100125.3	290.65	49.7	198319.4	397633.7
Inlet device with the softest sieve	17	99991.98	290.29	50.0	213852.3	428407.3
PARAMETER	p_{2t}	p_3	p_4	T_{2t}'	T_{2t}	T_{3t}
UNIT	Pa	Pa	Pa	K	K	K
Inlet device without a sieve	351178.4	351524.7	128716.5	458.35	459.55	1169.25
Inlet device with a soft sieve	351571.5	351462.6	128977.1	458.45	459.95	1170.05
Inlet device with a basic sieve	351971.5	351326.2	154655.8	458.55	460.25	1170.35
Inlet device with a dual sieve	366122.2	340125.3	154192.9	460.65	461.95	1172.95
Inlet device with the softest sieve	400157.2	327326.2	153674.3	470.01	471.15	1261.65
PARAMETER	T_{4t}	Q_{fuel}	G_{fuel}	c_h	F_T	c_m
UNIT	K	cm^3/cycle	kg/cycle	$kg.h^{-1}$	N	$kg.h^{-1}N^1$
Inlet device without a sieve	1039.15	1407	1.09045	77.0065	732.5*	0.105128*
Inlet device with a soft sieve	1041.15	1405	1.0889	78.8700	731.6*	0.107811*
Inlet device with a basic sieve	1043.45	1397	1.0819	75.2900	698.1*	0.107847*
Inlet device with a dual sieve	1085.65	1330	1.0312	74.7434	598.7*	0.125334*
Inlet device with the softest sieve	1216.65	1293.3	1.0027	72.6600	541.1*	0.13428*

* Calculated parameter.

1. Throttling of an input device of MPM - 20 changes parameters in the engine, their character is the same as the change in a coefficient of maintaining the total air pressure in the intake device σ_{intake}.
2. The throttling of the inlet device of MPM - 20, from the thermodynamic parameters, mostly effects the static pressure of the gas behind the gas turbine p_4 (-19.39 %), the total temperature of the gas behind the gas turbine T_{4t} (-17.081 %), total air pressure behind the compressor p_{2t} (-13.95 %), total gas pressure the in front of the gas turbine T_{3t} (-7.903 %) and a total air temperature behind the compressor T_{2t} (-2.524 %).
3. Throttling input device MPM - 20 leads to a higher operating point convergence to the limit in the characteristics of unstable labor centrifugal compressor.
4. Despite higher resistance of the radial compressor of MPM - 20 comparing to against unstable work was the seventh measurement with 83 % throttling of the inlet system to its unstable work and destruction of gas turbine blades and burn of the sealant mass in the body of the gas turbine above the rotor blades.

Changing of the inlet flow cross-section to the ATCE and GT radial compressors has a significant effect on its thermodynamic and performance parameters. When In case of large throttling or sudden reductions in air flow through the input device, unstable flow may affect a specific area or the entire radial compressor, which may cause damage to the ATCE gas turbine (Fig. 14, 15). [11]

4. LITERATURE LIST

[1] HOCKO M.: „Assessment of the ATCE State Based on Changes in Thermodynamic Parameters“, thesis, VLA Košice 2003, pp. 338

[2] RŮŽEK, J.: „Theory of Aircraft Engines, Part I (Compressors, Turbines and a Combustion Chamber)“, University textbook VA AZ Brno 1979, pp. 373

[3] OTT, A.: „Fundamentals of the Theory and Design of Air Vane Engines, Part I“, University Textbook, Military Academy of Aviation, Kosice 1983, pp.140

[4] MED, S.: „Diagnosis of JE - TS -20 in Laboratory Conditions K – 316“, master's thesis, Department of Aircraft, Military academy in Brno

[5] CUMPSTY, NA, „Compressor aerodynamics”, Department of Engineering University of Cambridge,1989, pp. 687

[6] HOCKO, M., GAŠPAR, R., 2013, „Impact of rapid thermal fluctuations of the airflow into engine inlet to the gas-dynamics stability of the turbojet engine“, 12th conference Power System Engineering, Thermodynamics& Fluid Flow, Pilsen. 2013, pp. 8

[7] HOCKO M.: „The small jet engine MPM – 20“, VLA Kosice

[8] ЧЕРКЕЗ, А., Я.: „Инжинерные расчеты газотурбиных двигателей методом малых одклонений“, Издательство Машиностроиение, 1975, pp. 379

[9] „The operation and maintenance of the engine AL - 7F - 1 , Book 2 , Book 3, Let -21 -20/2, Let – 21 -20/ 3“, Praha 1965

[10] FŐZŐ, L., ANDOGA, R., MADARÁSZ, L., „Mathematical model of a small Turbojet Engine MPM – 20“. In: Studies in Computational Intelligence.Vol . 313, 2010, p. 313-322

[11] HOCKO M., POLANSKÝ, J.: Experimental modelling of unstable operation of a centrifugal compressor on a small jet engine in the laboratory. 11th. World Congress on Computational Mechanics, 5th. European Conference on Computational Mechanics, 6th. European Conference on Computational Fluid Dynamics: 20. - 25.7.2014: Barcelona

[12] HOCKO M., POLANSKÝ, J.: Transformation of an aviation turboshaft engine into a experimental jet engine for laboratory testing unstable radial compressor work. Proceeding of the ASME 2014 International Techanical Engineering Congress & Exposition IMECE 2014 November 14-20, 2014, Montreal, Quebec, Canada